Neurotoxicity Research
https://doi.org/10.1007/s12640-021-00435-w

ORIGINAL ARTICLE

Resveratrol Inhibits NLRP3 Inflammasome-Induced Pyroptosis and miR-155 Expression in Microglia Through Sirt1/AMPK Pathway

Kemal Ugur Tufekci[1] · Bedir Irem Eltutan[2,3] · Kamer Burak Isci[4] · Sermin Genc[2,4]

Received: 1 June 2021 / Revised: 23 October 2021 / Accepted: 25 October 2021

Abstract

Resveratrol is a natural polyphenolic compound with a wide range of biological activities such as antioxidant, anti-carcinogenic, anti-obesity, anti-aging, anti-inflammatory, immunomodulatory properties. Accumulating evidence suggests that resveratrol has pharmacological benefits in life-threatening diseases, including cardiovascular disease, cancer, diabetes, and neurodegenerative diseases. Resveratrol is widely known for its anti-inflammatory properties; however, signaling mechanisms of anti-inflammatory action are still elusive. Studies have illustrated that resveratrol can control different regulatory pathways by altering the expression and consequently regulatory effects of microRNAs. Our study aims to clarify the regulatory mechanisms of resveratrol in its anti-inflammatory features in the N9 microglial cell line. Our results demonstrated that resveratrol inhibits LPS- and ATP-activated NLRP3 inflammasome and protects microglial cells upon oxidative stress, proinflammatory cytokine production, and pyroptotic cell death resulting from inflammasome activation. Additionally, resveratrol inhibits nuclear factor kappa-light-chain-enhancer of activated B cells (NF-κB) signaling and activates AMPK/Sirt1 pathways. Furthermore, our results indicated that resveratrol downregulated inflammasome-induced miR-155 expression. Then, inhibition of AMPK and Sirt1 pathways has significantly reversed protective effect of resveratrol on miR-155 expression. To sum up, our results suggest that resveratrol suppresses the NLRP3 inflammasome and miR-155 expression through AMPK and Sirt1 pathways in microglia.

Keywords Resveratrol · NLRP3 inflammasome · Microglia · Sirt1 · AMPK · microRNA

Introduction

Microglia are the resident innate immune cells in the central nervous system (CNS) responsible for homeostasis, phagocytosis of cellular debris or pathogens, and the secretion of cytokines and chemokines (Walter et al. 2017). Microglial activation, the brain's primary defense mechanism, occurs due to pathogens, brain injury, or neurotoxins (Lee et al. 2019; Tang and Le 2016). They are activated through Toll-like receptors (TLRs) and NOD-like receptors (NLRs) to mediate neuroinflammatory responses by producing and secreting proinflammatory cytokines and mediators (Hanamsagar et al. 2012). Inflammatory mediators from microglia amplify the neuroinflammatory responses in CNS via innate immune activation mechanisms, such as inflammasomes.

NLRP3 (NOD-, LRR-, and pyrin domain-containing protein 3) inflammasome, a part of the innate immune system, is a multi-protein complex that triggers proinflammatory responses. Activation of NLRP3 can be caused by pathogen-associated molecular patterns (PAMPs), such as microbiological insults and danger-associated molecular patterns (DAMPs), like adenosine triphosphate (ATP), reactive oxygen species (ROS), and peptide aggregates via RIG-like receptors (RLRs), C-type lectin receptors, purinergic receptors, TLRs, and NLRs (Heneka et al. 2018). Upon activation through PAMPs or DAMPs, NLRP3 oligomerizes with the

These authors contributed equally to this work: Kemal Ugur Tufekci and Bedir Irem Eltutan.

✉ Sermin Genc
sermin.genc@deu.edu.tr

[1] Department of Health Care Services, Vocational School of Health Services, Izmir Democracy University, 35290 Izmir, Turkey

[2] International Biomedicine and Genome Center, Balcova 35340 Izmir, Turkey

[3] Izmir International Biomedicine and Genome Institute, Dokuz Eylul University, Izmir, Turkey

[4] Department of Neuroscience, Health Science Institute, Dokuz Eylul University, Izmir, Turkey

Published online: 05 November 2021

apoptosis-associated speck-like protein containing CARD (ASC) and pro-caspase-1 to form an inflammasome complex (Herman and Pasinetti 2018). Following inflammasome complex formation, interleukin-1β (IL-1β) and interleukin-18 (IL-18) are cleaved by caspase-1 of inflammasome complex and released to extracellular space (Heneka et al. 2018). Activated caspase-1 also modulates cleavage of Gasdermin D (GSDMD) from its N terminal, which forms pores at the cell membrane, and causes IL-1β and IL-18 secretion and water molecule inflow, resulting in pyroptotic cell death as a result of osmotic cell denaturation (Shi et al. 2015). Activation of the NLRP3 inflammasome cascade may also mediate neuroinflammatory processes implicated in many neurological diseases like Alzheimer's disease, Parkinson's disease, traumatic brain injury, stroke, depression, and multiple sclerosis (Heneka et al. 2018; Hung et al. 2020; Kaufmann et al. 2017). Against inflammasome-associated neurodegenerative diseases, phytochemicals can be utilized to suppress inflammasome activation as therapeutics agents.

Resveratrol (3,5,4′-trihydroxy-trans-stilbene, RSV), a non-flavonoid polyphenolic compound, is especially abundant in the skin red of grapes (Lu et al. 2010; Thiel and Rossler 2016). RSV is extensively studied for its cardioprotective and cancer preventive roles (Thiel and Rossler 2016). Furthermore, it is well-known for its antioxidant, anti-aging, and anti-inflammatory effects. Previous studies have shown that RSV may have protective effects in the central nervous system against neuroinflammation (Sui et al. 2016). It reduces the synthesis of proinflammatory mediators and induces anti-inflammatory proteins, which result in anti-inflammatory effects. Several lines of evidence have shown that RSV can suppress inflammasome activation in various tissues and organs, including the brain (Olcum et al. 2020a). RSV inhibits inflammasome activation and subsequent behavioral changes in the animal model of neurodegeneration induced by amyloid-β (Qi et al. 2019), in which protective roles are mediated by SIRT1 and AMPK and protects microglial cells against amyloid-β induced inflammasome activation via supressing TXNIP/thioredoxin/NLRP3 (Feng and Zhang 2019). Furthermore, in animal model estrogen deficiency-induced depression, RSV upregulated SIRT1 in hippocampal dentate gyrus resulting in diminished depressive- and anxiety-like behaviors (Liu et al. 2019). However, previous work has failed to address whether RSV mediates post-transcriptional modifications to regulate NLRP3 inflammasome activation.

MicroRNAs (miRNAs) are 22-nucleotide small RNA molecules that mediate gene expression regulation at the post-transcriptional level by selectively binding to recognition sites in 3′-UTR of target mRNAs to suppress the initiation of translation or progression of mRNA degradation (Grosshans and Filipowicz 2008; Erson-Bensan 2014; Tufekci et al. 2014). miRNAs play various regulatory roles in cell proliferation, differentiation, apoptosis, signal transduction, organ development, and the development and functioning of the immune system (Tufekci et al. 2014). In the immune system, miRNAs have multifaceted roles affecting pro- and anti-inflammatory processes upon inflammatory stimuli. The primary regulator miRNAs are miR-146a and miR-155, regulated by NF-κB activation in immune cells (O'Connell et al. 2007; Tili et al. 2007; Cardoso et al. 2016). Furthermore, other miRNAs, namely miR-132 and miR-125b, modulate innate and adaptive immune responses. Of these, miR-155 and miR-132 have extensive proinflammatory effects, whereas miR-125b and miR-146a are mostly negative regulators of inflammation (Tufekci et al. 2014). Several studies have shown that neurological disorders cause the upregulation of miR-155 in microglia, thereby differentiation of microglia into the M1 phenotype through regulation of signaling pathways. Based on what we know, RSV can downregulate miR-155 and provide the differentiation of microglia into the M2 phenotype in the favor of anti-inflammatory diseases (Ghazavi et al. 2020). A recent study has revealed that miR-155 expression regulates NLRP3 inflammasome activation (Artlett et al. 2017). In addition to miR-155, inflammasome activation is regulated by miR-223, which directly targets the 3′-UTR region of NLRP3 mRNA (Bauernfeind et al. 2012). Thus, identifying regulatory molecules modulating NLRP3 inflammasome is beneficial to understand the mechanism of the inflammasome in responses to neurodegeneration and to clarify beneficial candidates for new therapeutic approaches.

RSV is a potent candidate for the treatment of neuroinflammatory diseases due to the ability to cross the blood–brain barrier and the presence of versatile effects. Furthermore, RSV also inhibits inflammasome activation in the nervous system. This study aims to clarify the signaling pathways in which RSV has anti-inflammatory properties on suppressing NLRP3 inflammasome and the mechanisms of controlling these signaling pathways. The present study showed that RSV inhibits NLRP3 inflammasome activation and microglial cell death in LPS- and ATP-stimulated murine N9 microglial cells.

Methods

Chemicals and Reagents

Cis-Resveratrol (Cat#: ab144436) was obtained from Abcam (UK). RPMI 1640 medium, L-glutamine, penicillin/streptomycin, phosphate-buffered saline (PBS), and trypsin/EDTA were purchased from Biochrom (Germany). Fetal bovine serum (FBS) (Cat#:10,500,064) was purchased from Gibco (USA). Propidium iodide (Cat#: P1304MP) was purchased from Thermo Scientific (USA). Lipopolysaccharide (Cat#:tlrl-3pelps) was purchased from Invivogen (USA).

Adenosine 5′-triphosphate disodium salt hydrate (Cat#: A6419-1G), compound C (Cat#: P5499), and Ex527 (Cat#: E7034) were purchased from Sigma-Aldrich (USA).

Cell Culture and Treatments

Mouse microglial cell line N9, generously supplied from Dr. Paola Ricciardi-Castagnoli (Cellular Pharmacology Center, Milan, Italy), was cultured at 37 °C in a humidified incubator with 5% CO_2–95% air environment (Righi et al. 1989). Cells were maintained in RPMI 1640 supplemented with 2 mM L-glutamine, 10% fetal bovine serum (FBS), 100 U/ml penicillin, and 100 µg/ml streptomycin. All cell culture treatments were performed in serum-free RPMI 1640 medium supplemented with 2 mM L-glutamine. In our experimental inflammasome activation model, the cells were incubated with RSV (10 µM, 1 h), then ultra-pure LPS (1000 ng/ml, 4 h), followed by ATP (5 mM, 1 h). Treatments with inhibitors were carried out before the classical experiment model with AMPK inhibitor compound C (20 µM,1 h) and SIRT1 inhibitor Ex527 (20 µM, 1 h). All experiments were repeated 3 times, using 5 technical replicates. Passage number of N9 cells in study was between 40 and 60.

Cell Viability Assay

Cell viability was determined using a tetrazolium-based colorimetric assay, namely CCK-8 (Cell counting kit-8, Sigma-Aldrich, St Louis, USA). N9 cells (1×10^4/well) were seeded into 96-well plates and incubated overnight. After treatments, 10 µl of WST-8 solution was added to each well and incubated for 2 h at 37 °C. Absorbance was measured at 450 nm with a reference wavelength of 630 nm using a microplate reader (Varioskan, Thermo Scientific, USA). Cell viability was expressed as a percentage of the untreated cells.

Cytotoxicity Assay

Cells were treated with LPS (1 µg/ml) for 4 h and then ATP (5 mM) for 1 h with or without 1 h RSV pre-incubation. After treatments, cell-free supernatant was collected, and the release of lactate dehydrogenase (LDH) was analyzed spectrophotometrically by LDH Cytotoxicity Detection Kit (Roche, Basel, Switzerland) according to the manufacturer's guidelines. Each well's absorbance was measured at 492-nm wavelength with a reference wavelength at 630 nm on a microplate reader. Cell cytotoxicity was expressed as the percentage of the maximum LDH activity.

Propidium Iodide Staining

Cells were seeded into 48-well plates with a density of 3×10^4 cells per well. Fifteen minutes before the end of treatment, propidium iodide (PI) was added each well to the final concentration of 50 µg/ml in the dark and incubated for 15 min. A phase-contrast microscope (Olympus IX71, Japan) was used to detect dead cells marked by PI stain (PI-positive cell). PI-positive cells were counted by ImageJ (National Institutes of Health, USA) software (Schneider et al. 2012), and data were shown as the percentage of total cells.

Enzyme-Linked Immunosorbent Assay (ELISA)

Microglial cells (5×10^4/well) were seeded into 96-well plates and cultured overnight. Following treatments, cell culture supernatants were collected for the measurement of IL-1β and IL-18. The level of IL-1β in the culture medium was measured using the IL-1β ELISA kit (eBioscience, USA), and IL-18 levels were detected using mice IL-18 ELISA Kit (eBioscience, USA) following the manufacturer's protocol.

Caspase-1 Activity Assay

Murine microglial cells (1×10^4/well) were seeded into 96-well plates and incubated overnight. In vitro experimental model was applied with or without specific AMPK and Sirt1 inhibitors. Following the treatments, the samples' supernatant was taken into a white-walled 96-well plate, and Caspase-1 activities were determined via luminometric Caspase-Glo-1 Inflammasome Assay (Promega, USA) according to manufacturer's protocol using Centro XS3 lb 960 microplate luminometer (Berthold Technologies, Germany).

Immunofluorescence Staining for ASC Specks

Microglial cells were seeded into 25cm^2 flasks with a density of 1×10^6 cells per flask. Following the treatment, cells were fixed with 4% paraformaldehyde in PBS and permeabilized with 0.2% Triton X-100 in PBS and washed twice. Permeabilization and blocking were performed with PBS containing 10% FBS and 0.5% Triton-X-100 at 37 °C for 30 min. Cells were incubated with ASC primary antibody (Santa Cruz Biotechnology, sc-33958, 1:100 diluted) overnight, and Alexa Fluor-488 conjugated the Anti-goat antibody (Jackson Immunoresearch, 705–545-003, 1:1000) for 1 h. ASC speck images were obtained under LSM 880 Confocal microscopy (Zeiss, Germany). ASC speck positive cells were counted by ImageJ, and data were expressed as a percentage of total cells.

Intracellular ROS Detection

Murine microglial cells (1×10^4/well) were seeded into 96-black-well plates and incubated overnight.

Following the treatments, microglial cells were treated with 2′,7′-dichlorofluorescein diacetate (CM-H_2-DCFDA), the ROS sensor, was incubated for 1 h. The fluorescence intensity of each well in the plate was measured by 495-nm excitation and 532-nm emission by Varioskan Flash (Thermo Scientific, USA) fluorescence plate reader. Fluorescence values of the samples were normalized to control groups and analyzed quantitatively.

Mitochondrial ROS Detection

The assay was performed both immunocytochemically and fluorometrically. For the immunocytochemical procedure, 3×10^4 cells per well were seeded in 48-well plates and incubated overnight. After the inflammasome activation was carried on, MitoSOX (5 µM) and Hoechst 33,342 dye (20 µM) were added to the wells for 10 min. Images of cells were taken via an inverted fluorescent microscope (Olympus IX-71, Japan). For the fluorometric procedure, murine microglial cells (1×10^4/well) were seeded into 96-black-well plates and incubated overnight. After incubation, the experimental inflammasome activation model was applied. Mitochondrial ROS production in N9 cells was measured using MitoSOX (Molecular Probes, Invitrogen, USA) staining (to a final concentration of 5 µM for 15 min at 37 °C). The MitoSOX fluorescence (Ex 530 nm/Em 590 nm) was measured using a Varioskan Flash (Thermo Scientific, USA) fluorescence plate reader.

Real-Time PCR Analysis of mRNAs

Total RNA was extracted from N9 cells using the Nucleospin RNA II Kit (Macherey–Nagel, Germany) according to the manufacturer's instructions. Reverse transcription was performed using Revert-Aid First Strand cDNA Synthesis Kit (Thermo, USA). Quantitative real-time PCR was performed using GoTaq qPCR Mastermix (Promega, USA) and LightCycler 480 Instrument II (Roche Life Science, USA) following the manufacturer's protocol. The primers used in the qPCR reactions are listed in Table 1. PCR amplification of the template cDNAs was performed for 40 cycles using the following conditions: initial denaturation at 95 °C for 10 min, temperature cycling of denaturation at 95 °C for 10 s, annealing at 60 °C for 10 s, and extension at 72 °C for 20 s was performed. The specificity of PCR products was determined by the melting curve analysis. The relative expression levels of mRNAs were quantified using the $2^{-(\Delta\Delta Ct)}$ method with endogenous normalization to the average amounts of the housekeeping gene, glyceraldehyde 3-phosphate dehydrogenase (*GAPDH*) (Livak and Schmittgen 2001).

Real-Time PCR Analysis of miR-155

Total RNA was isolated with miRNeasy mini kit (Qiagen, Germany), and cDNAs were synthesized by miScript RT II (Qiagen, Germany) kit. Real-time qPCR was performed using the miScript SYBR Green PCR Kit (Qiagen, Germany) on a Lightcycler® 480 Real-Time PCR System (Roche Diagnostics, Germany). Primers for mature miR-155 and housekeeping genes U6 and SNORD95 were purchased from Qiagen (Valencia, CA). Changes in miRNA levels were measured by the threshold cycle ($\Delta\Delta C_T$) method (Livak and Schmittgen 2001).

Western Blot

Cells were seeded into T75 cell culture flasks with a density of 3×10^6 cells and incubated overnight. Following the treatments, cells were harvested via scrapper, and total protein was isolated from cells with RIPA lysis solution containing protease and phosphatase inhibitor (Thermo Scientific, USA). For cytosolic and nuclear protein fractionation, NE-PER Nuclear and Cytoplasmic Extraction Reagent (Thermo Scientific, USA) was used following the manufacturer's protocol. Protein concentrations were determined by Bicinchoninic Acid Kit for Protein Determination (Santa Cruz, USA). An equal amount of proteins were separated by 8–15% SDS-PAGE gel and transferred to a PVDF membrane. Then, membranes were incubated in a blocking buffer, BSA, or milk with the required percentages within the TBST washing solution for 1 h. After blocking, the

Table 1 List of PCR primers

mRNA		Sequence (5′–3′)	Product length	Accession number
IL-1β	Forward	TTCTTTTCCTTCATCTTTGAAGAAG	365 bp	NM_008361.4
	Reverse	TCCATCTTCTTCTTTGGGTATTGTT		
IL-18	Forward	CTTTGGAAGCCTGCTATAATCC	363 bp	NM_008360.2
	Reverse	GGTCAAGAGGAAGTGATTTGGA		
NLRP3	Forward	TGCCTGTTCTTCCAGACTGGTGA	143 bp	NM_145827.4
	Reverse	CACAGCACCCTCATGCCCGG		
GAPDH	Forward	ACCACAGTCCATGCCATCAC	452 bp	NM_001289726.1
	Reverse	TCCACCACCCTGTTGCTGTA		

membranes were incubated overnight at 4 °C with primary antibodies (Table 2), specified for the desired protein according to antibodies protocol. Membranes were incubated with the horseradish peroxidase (HRP)–conjugated secondary antibodies and chemiluminescent Supersignal West Dura ECL reagent (Thermo Scientific, USA) was used for imaging, and images were taken with Chemi-Smart 5100 (Vilber Lourmat, France). Band intensities were evaluated densitometrically with ImageJ (Schindelin et al. 2015).

miRNA Transfection

In order to unravel the role of miR-155 in the protective roles of RSV, functional assays with miR-155 mimic were performed. For this experiment, N9 cells were seeded into T25 cell culture flasks with a density of 1.5×10^5 cells in an antibiotic-free growth medium and incubated overnight. Then, the cells were transfected with miR-155 mimic (50 µM) or negative control mimic (AllStars Negative Control siRNA, 50 µM) for 48 h with HiperFect Transfection reagent (Qiagen, Germany) according to manufacturer's recommendations.

Statistical Analysis

For statistical analyses, GraphPad Prism 9.0.1 (GraphPad Software Inc., CA, USA) was used. The normality of data was analyzed with the Shapiro–Wilk test. For groups more than two, one-way ANOVA with Sidak's multiple comparisons test was performed in the case of normal distribution. In order to compare two experimental groups, Mann–Whitney *U*-test was utilized. Data are presented as mean ± SEM, and $p < 0.05$ was considered statistically significant.

Table 2 Primary antibodies

Antibody	Provider	Catalog Number	Dilution
Anti-IL-1β	Abcam	ab9722	1:1000
Anti-Caspase-1	Abcam	ab1872	1:1000
Anti-NLRP3	Adipogen	AG-20B-0014	1:1000
Anti-Sirt1	Cell Signaling	8469S	1:1000
Anti-p-AMPKα (Thr172)	Cell Signaling	2535S	1:1000
Anti-AMPKα	Cell Signaling	2532S	1:1000
Anti-Gasdermin D	Abcam	ab209845	1:500
Anti-NF-κB p65	Santa Cruz	sc-372	1:1000
Anti- IκBα	Cell Signaling	9242S	1:1000
Anti-β-actin	Abcam	ab8227	1:1000
Anti-Lamin A/C	Santa Cruz	sc-20681	1:1000
Anti-Rabbit HRP Secondary	Cell Signaling	7074	1:2000
Anti-Mouse HRP Secondary	Cell Signaling	7076	1:2000

Results

RSV Inhibited LPS- and ATP-Induced Secreted Levels and mRNA Expressions of IL-1β and IL-18 in Microglial Cells

Before investigating the effect of RSV on microglia NLRP3 inflammasome activation, we evaluated a non-toxic RSV dose with cytotoxicity assay. RSV has caused no cytotoxicity on N9 microglial cells up to 50 µM concentration (Fig. 1A). To investigate the effect of RSV on NLRP3 inflammasome-related cytokines IL-1β and IL-18 in microglial cells, they were treated by LPS and ATP. Then, we analyzed secreted cytokine levels upon LPS and ATP treatment with or without RSV pre-treatment. ELISA analysis has presented that RSV significantly inhibited IL-1β and IL-18 secretion induced by LPS and ATP (Fig. 1B, C). Similarly, quantitative real-time PCR analyses showed that LPS and ATP treatment enhanced mRNA expressions of cytokines while RSV decreased IL-1β and IL-18 mRNA expression levels (Fig. 1D, E). We next evaluated whether the RSV affected secreted and intracellular IL-1β protein levels. Our Western blot analysis indicated that RSV pre-treatment dramatically decreased both pro-IL-1β and mature IL-1β levels (Fig. 1F–H).

RSV Inhibits NLRP3 Inflammasome

The NLRP3 inflammasome is a type of NLR, a known protein complex consisting of NLRP3, ASC adaptor protein, and caspase-1. We first evaluated the caspase-1 protein levels. We determined no significant difference in the intracellular level of caspase-1 p45 among experimental groups (Fig. 2A, B). However, RSV significantly reduced active caspase-1 p20 compared to LPS- and ATP-treated cells (Fig. 2A, C). Next, we examined NLRP3 expression at mRNA and protein levels. RSV significantly decreased the expression of NLRP3 both in mRNA and protein levels, which was increased with LPS and ATP induction (Fig. 2D–F). Furthermore, our immunofluorescence staining results revealed that RSV attenuated ASC speck formation induced by LPS and ATP (Fig. 2G, H).

RSV Prevented Pyroptotic Cell Death and Cleavage of Gasdermin D in LPS- and ATP-Treated Microglial Cells

The effect of RSV pre-treatment on cell death by administration of LPS and ATP was first determined via LDH assay. According to our results, LPS and ATP dramatically increased cell death in N9 cells, while RSV pre-treatment significantly decreased the cytotoxicity (Fig. 3A). Similarly,

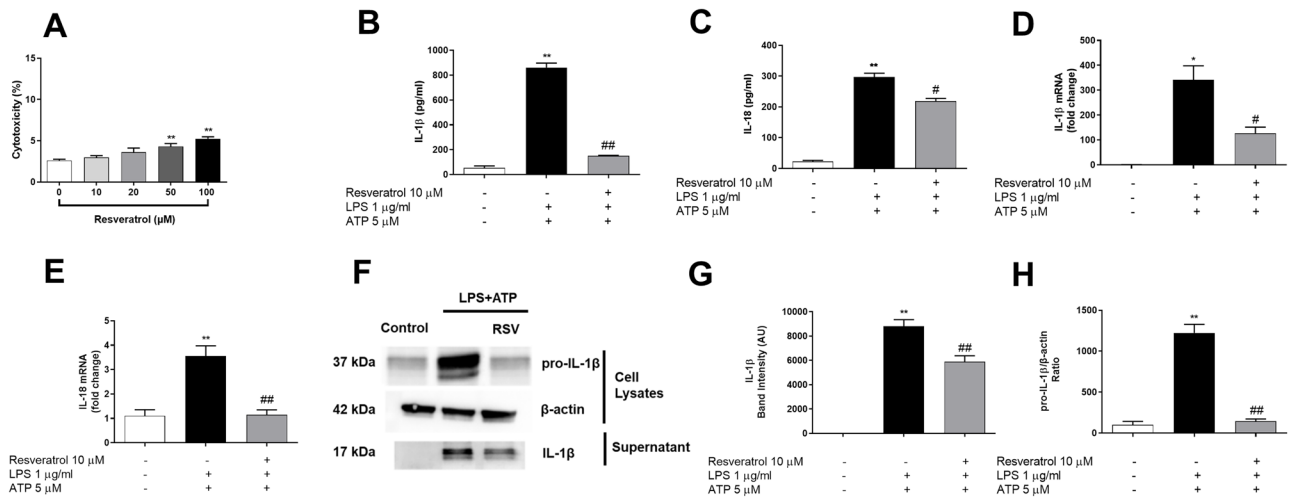

Fig. 1 RSV reduced mRNA and protein levels of IL-1β and IL-18. N9 microglial cells were pre-treated with RSV (10 μM) for 1 h, then treated with LPS (1 μg/ml) for 4 h and ATP (5 mM) for 1 h. (**A**) The toxicity of RSV is determined. (**B**, **C**) The suppressor effect of RSV on secreted IL-1β and IL-18 was measured with ELISA. (**D**, **E**) mRNA levels of IL-1β and IL-18 reduced by RSV pre-treatment compared to LPS and ATP induction group. (**F**, **G**, **H**) RSV reduced protein levels of pro-IL-1β and secreted IL-1β compared to LPS- and ATP-induced cells. The results are presented as mean ± S.E.M, $n = 5$. $^{*}p < 0.05$, $^{**}p < 0.01$ compared to control and $\#p < 0.05$, $\#\#p < 0.01$ compared to LPS and ATP treated cells

cell viability assay showed that RSV increased cell viability in LPS- and ATP-induced microglial cells (Fig. 3B). The effect of RSV on pyroptotic cell death was demonstrated by propidium iodide (PI) staining and western blot analysis of GSDMD. LPS and ATP treatment enhanced the number of PI-positive cells; however, RSV significantly suppressed LPS- and ATP-induced cell death (Fig. 3C, D). It has been known that pyroptosis displays plasma membrane disruption. In pyroptotic cell death, the cell's nucleus is located in the center and above the main plane of the cell body. These cells often resemble to a fried egg (Chen et al. 2016). To address these typical morphological features, we took phase-contrast images. These signs can be clearly observed in the cell with pyroptotic cell death (Fig. 3E). Next, our Western blotting analysis revealed that pre-treatment with RSV significantly reduced cleaved GSDMD levels compared to the LPS- and ATP-treated group (Fig. 3F, G).

RSV Ameliorated Intracellular and Mitochondrial ROS Production

The intracellular ROS level in microglial cells was determined by DCFDA. Cellular ROS level in RSV pre-treated group was significantly decreased compared to the LPS and ATP group (Fig. 4A). To investigate mitochondrial ROS production, we examined MitoSOX analysis. The mitochondrial superoxide significantly increased within the cell via LPS and ATP induction. As shown in Fig. 4B–D, the fluorescence level was decreased in RSV preincubated cells.

RSV Inhibited NF-κB Translocation

The effect of RSV on nuclear translocation of NF-κB protein was investigated by Western blotting. Our blot revealed that LPS and ATP induction increased the band intensity of NF-κB protein. Pre-treatment with RSV showed a reverse effect and significantly decreased the NF-κB protein level. In addition, LPS and ATP treatment significantly increased the NF-κB protein level in the nucleus, and RSV pre-treatment significantly prevented this increase. Meanwhile, NF-κB protein level decreased in cytosolic samples after LPS and ATP treatment and RSV treatment reversed the reduction and increased NF-κB protein level in cytosolic samples (Fig. 5A). According to these results, LPS and ATP treatment significantly increased the ratio of nuclear to cytoplasmic NF-κB, and RSV pre-treatment decreased this ratio (Fig. 5B). Also, our blot showed that RSV pre-treatment significantly increased the IκBα band intensities which were decreased by LPS and ATP treatment (Fig. 5C, D).

RSV Activated SIRT1 and AMPK Pathways

To evaluate the mediator pathways in protective effects of RSV on NLRP3 inflammasome activation, we first investigated Sirt1 and AMPK pathways. The Western blot method was used to determine whether different doses of RSV (10 μM, 20 μM, and 50 μM) activated the Sirt1 and AMPK pathways. Our analysis has revealed that RSV treatment upregulated the band intensity of Sirt1 protein compared to the control group in a concentration-dependent manner

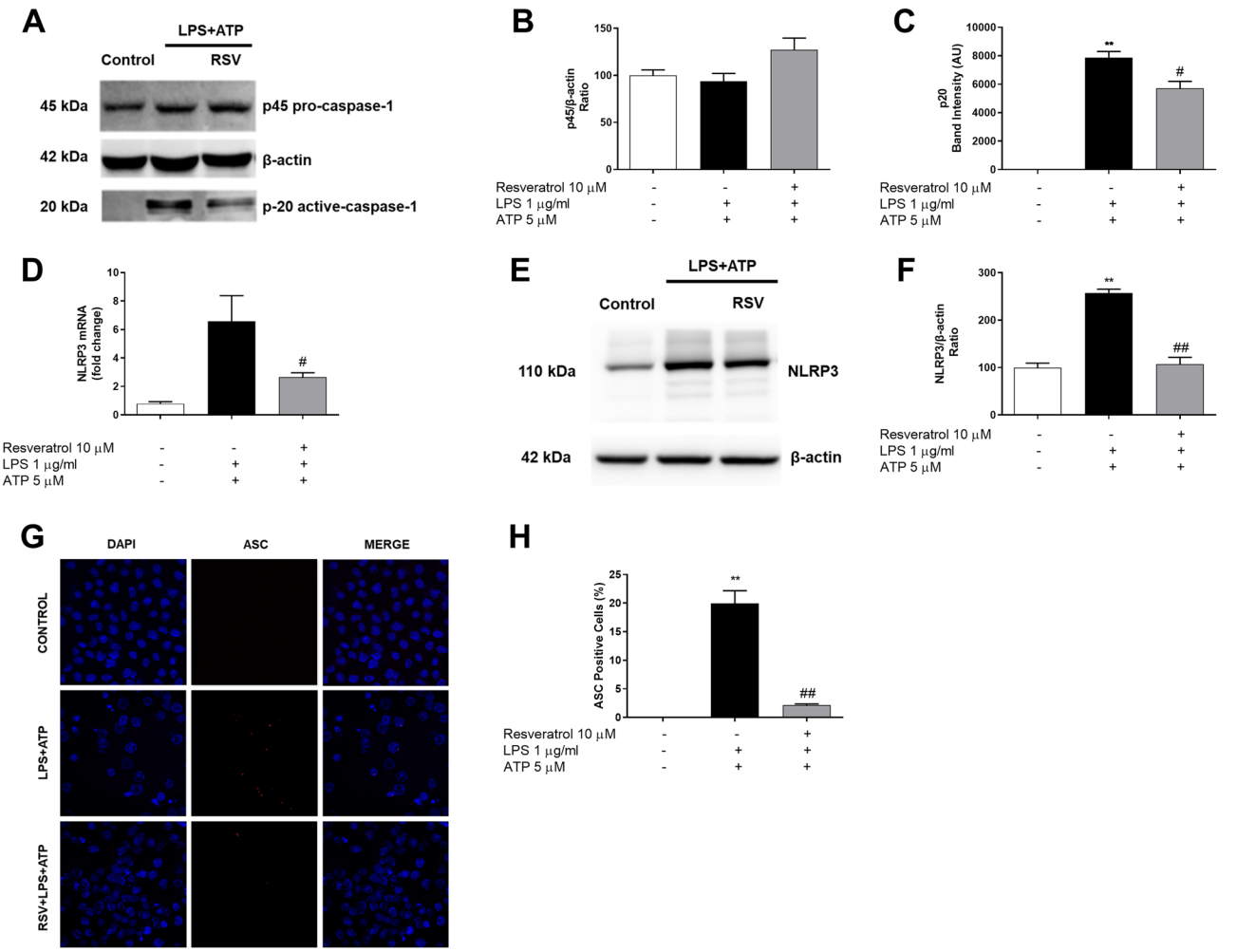

Fig. 2 RSV reduced NLRP3, caspase-1, and ASC speck formation. N9 microglial cells were pre-treated with RSV (10 μM) for 1 h, then treated with LPS (1 μg/ml) for 4 h and ATP (5 mM) for 1 h. (**A**, **B**, **C**) Pro-caspase-1 shows no difference among groups. RSV reduced cleaved caspase-1 in RSV pre-treated cells compared to LPS- and ATP-treated cells. (**D**, **E**, **F**) RSV suppressed NLRP3 on both protein and mRNA levels compared with LPS and ATP activated cells. (**G**) ASC speck formation was determined by confocal microscopy. (**H**) RSV significantly prevented ASC speck formation compared to LPS- and ATP-induced cells. The results are presented as mean ± S.E.M, $n = 5$. $*p < 0.05$, $**p < 0.01$ compared to control and $\#p < 0.05$, $\#\#p < 0.01$ compared to LPS- and ATP-treated cells

(Fig. 6A, B). Similarly, RSV treatment also increased the band intensity of AMPK phosphorylation in a dose-dependent manner (Fig. 6C, D).

Inhibition of SIRT1 and AMPK Activation Ameliorated Protective Effects by RSV Against NLRP3 Inflammasome Activation

To determine whether RSV utilizes its anti-inflammatory effects through Sirt1 and AMPK pathways, we checked the NLRP3 inflammasome activation by using inhibitors of these pathways. Western blotting analysis showed that Ex527 and CC reversed the effects of RSV on LPS- and ATP-induced cells, increasing the protein of NLRP3 (Fig. 7A, B). Inhibition of AMPK and Sirt1 pathways markedly raised both NLRP3 and IL-1β mRNA levels downregulated by RSV pre-treatment (Fig. 7C, D). Furthermore, pre-treatment with Ex527 and CC significantly elevated caspase-1 activity, which was diminished by RSV pre-treatment (Fig. 7E).

The miR-155 Level is Attenuated with RSV Treatment

First, transfection efficiency was determined by qPCR. miR-155 mimic transfection upregulated miR-155 over 1000-fold compared to the scrambled transfected group (Fig. 8A). To determine whether RSV suppresses the NLRP3 inflammasome by regulating the SIRT1 and AMPK pathways via miRNAs, we first examined RSV effects on the miR-155 expression level. Our qPCR analyses demonstrated that RSV pre-treatment

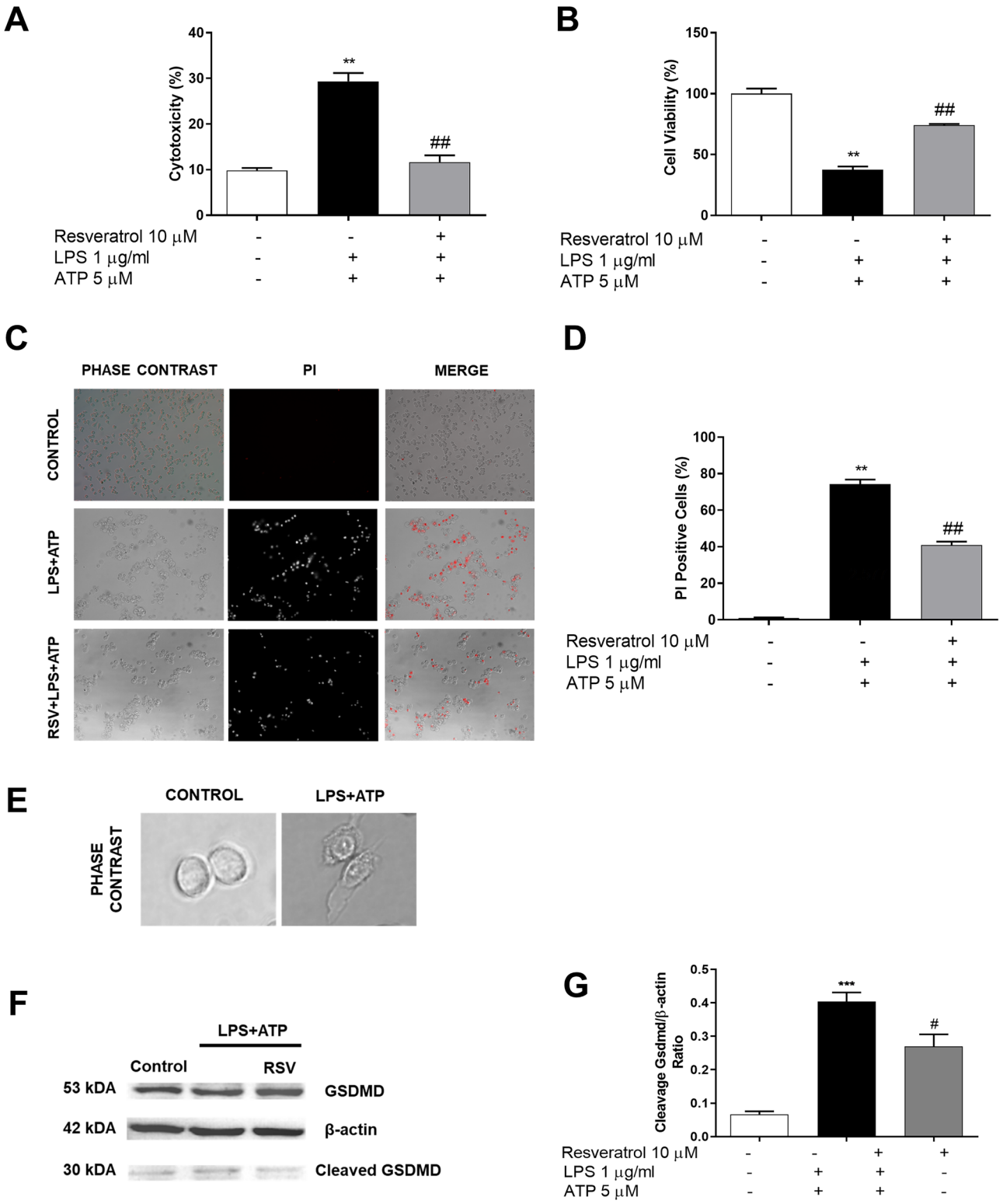

Fig. 3 RSV prevented pyroptotic cell death. N9 microglial cells were pre-treated with RSV (10 μM) for 1 h, then treated with LPS (1 μg/ml) for 4 h and ATP (5 mM) for 1 h. (**A**, **B**) Pre-treatment with RSV inhibited pyroptotic cell death and increased cell viability compared to LPS-and ATP-induced cells. (**C**, **D**) RSV reduced pyroptotic cell death and decreased PI-positive cells. (**E**) Phase-contrast image of control and LPS- and ATP induced-pyroptotic cells. (**F**, **G**) RSV ameliorated GSDMD cleavage induced by inflammasome activation. The results are presented as mean ± S.E.M, $n = 5$. *$p < 0.05$, **$p < 0.01$ compared to control and #$p < 0.05$, ##$p < 0.01$ compared to LPS- and ATP-treated cells

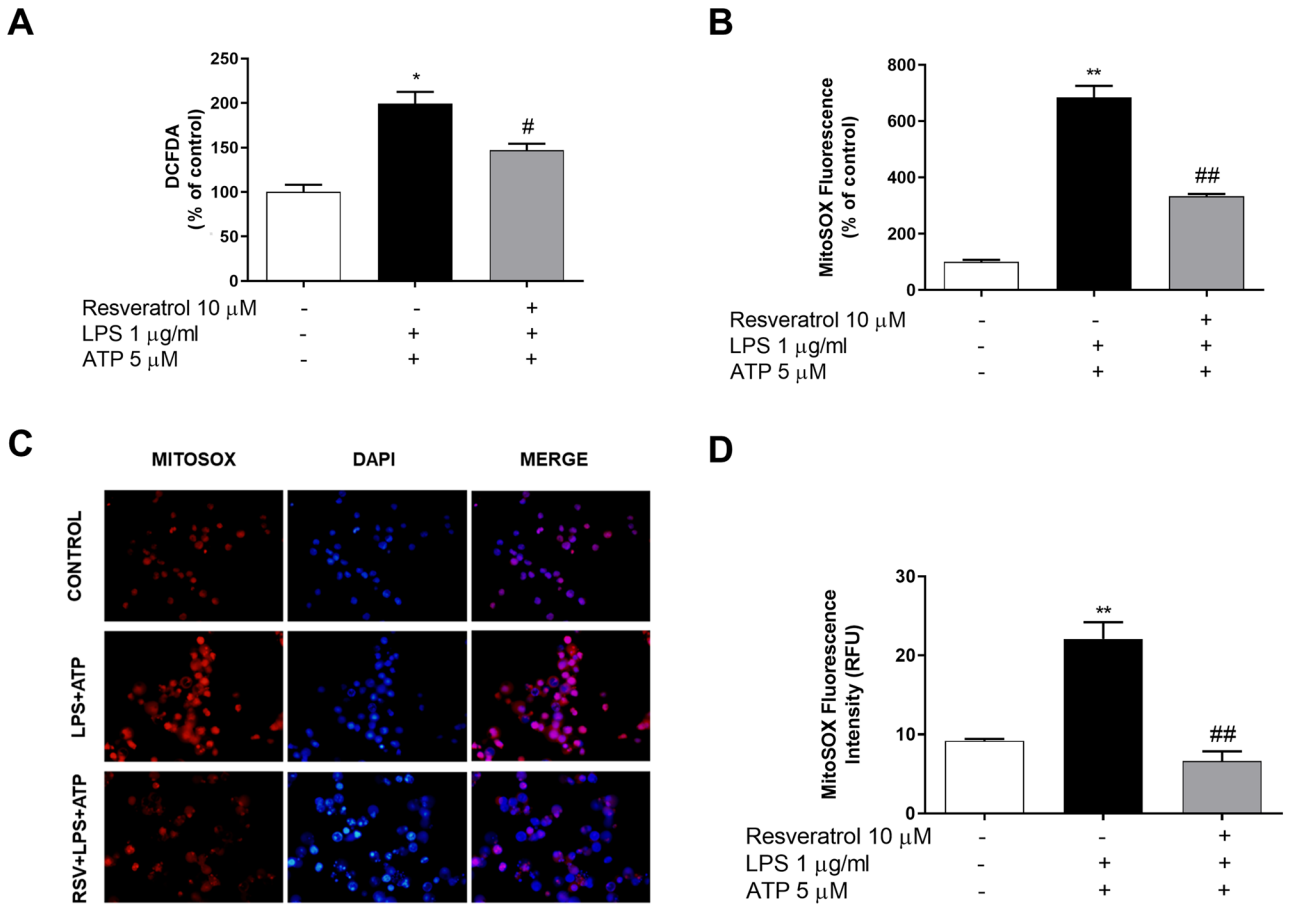

Fig. 4 RSV inhibited intracellular and mitochondrial ROS production. N9 microglial cells were pretreated with RSV (10 μM) for 1 h, then treated with LPS (1 μg/ml) for 4 h and ATP (5 mM) for 1 h. (**A**) RSV pre-treatment reduced intracellular ROS production. (**B**, **C**, **D**) RSV decreased mitochondrial ROS production compared with LPS- and ATP-activated cells in fluorometric measurements and cells were visualized with immunofluorescence. The results are presented as mean ± S.E.M, $n = 5$. *$p < 0.05$, **$p < 0.01$ compared to control and #$p < 0.05$, ##$p < 0.01$ compared to LPS- and ATP-treated cells

downregulated miR-155 level, upregulated by LPS and ATP induction in the N9 microglial cell line (Fig. 8B). The functional study with miR-155 mimics revealed that reversal of RSV suppressed protein levels of NLRP3 (Fig. 8C, D) and mRNA levels of NLRP3 (Fig. 8E), IL-1β (Fig. 8F), and IL-18 (Fig. 8G) compared to negative controls transfected groups. Furthermore, to establish which signaling pathways regulate suppression of miR-155 by RSV, we determined the miR-155 expression level with and without AMPK and SIRT1 inhibitors. Pre-treatment with CC and Ex527 reversed the downregulation of miR-155 expression significantly (Fig. 8G). These results have suggested that protective effects of RSV on miR-155 expression are dependent on AMPK and SIRT1 pathways.

RSV Treatment Rescued miR-155-Related Pyroptotic Cell Death

The effect of miR-155 mimic alone on pyroptotic cell death was assessed by propidium iodide (PI) staining. According to our results, miR-155 transfection dramatically increased cell death in N9 cells compared to scrambled transfected cells, while RSV pre-treatment significantly decreased the cytotoxicity (Fig. 9A, B).

Discussion

The NLRP3 inflammasome is an innate immune mechanism that plays a fundamental role in the pathogenesis of neurodegenerative diseases. Here, we demonstrated that RSV suppresses NLRP3 inflammasome and microglial pyroptosis by regulating the SIRT1 and AMPK pathways via miR-155. RSV is a well-known natural compound with its antioxidant, anticancer, anti-obesity, anti-aging, and anti-inflammatory effects (He et al. 2017). Previous clinical studies have concluded that the RSV dose range used in vitro is bioavailable for human administration (Espinoza et al. 2017; Movahed et al. 2013; Turner et al. 2015). Besides, its ability to interact with multiple

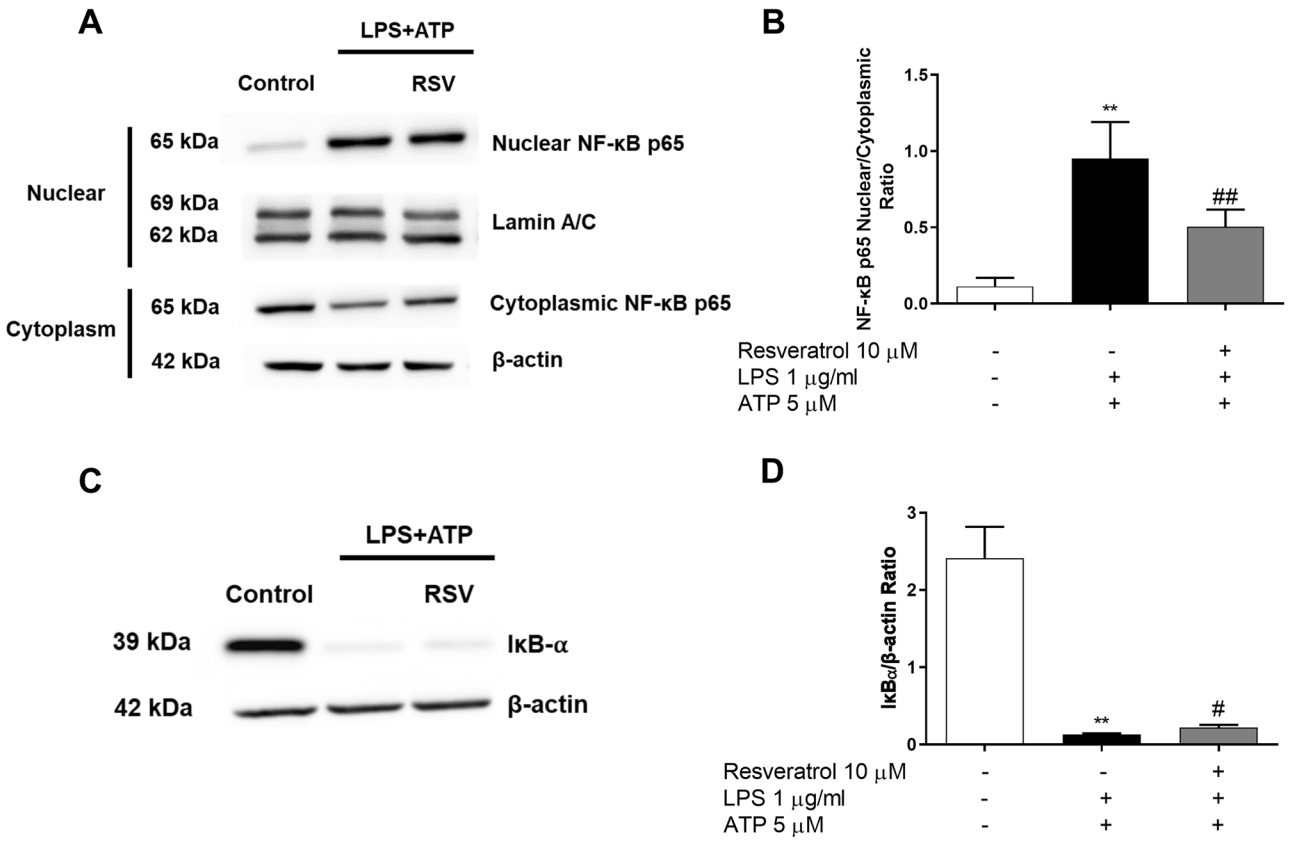

Fig. 5 RSV inhibited activation of NF-κB. N9 microglial cells were pre-treated with RSV (10 μM) for one hour, then treated with LPS (1 μg) for 30 min. (**A**, **B**) RSV rescued LPS and ATP induced an increase of nuclear/cytoplasmic ratio of NF-κB p65 subunit. (**C**, **D**) RSV pre-treatment significantly increased expression of IκBα, which is downregulated after LPS and ATP induction. The results are presented as mean ± S.E.M, $n = 5$. $*p < 0.05$, $**p < 0.01$ compared to control and $\#p < 0.05$, $\#\#p < 0.01$ compared to LPS- and ATP-treated cells

molecular targets involved in inflammation and immunity is well established. A growing body of literature has investigated the protective effects of RSV on neuroinflammation associated in vitro and in vivo models, such as sepsis-associated encephalopathy (Sui et al. 2016), experimental subarachnoid hemorrhage (Zhang et al. 2017), cerebral ischemia/reperfusion injury (He et al. 2017), and amyloid-β-induced cognitive decline (Qi et al. 2019). Previous studies on the neuroprotective roles of RSV mainly focused on its antioxidant, anti-inflammatory, and cytoprotective effects. RSV has been reported to ameliorate NLRP3 expression and IL-1β cleavage in hippocampus regions of sepsis-associated encephalopathy animal model (Sui et al. 2016). Another study has reported that RSV alleviated ischemia–reperfusion brain injury–induced NLRP3, caspase-1, IL- 1β, and IL-18 levels (He et al. 2017). Besides, RSV has also been revealed to be protective in experimental subarachnoid hemorrhage by suppressing NLRP3 and ASC expressions and cleavage of caspase-1, IL- 1β, and IL-18 (Zhang et al. 2017).

NLRP3 inflammasome activation occurs as a result of two different signals, namely priming and activation. While mRNA and protein levels of NLRP3 complex compounds are upregulated in the priming step, NLRP3 activation and inflammasome recruitment occur in the activation phase (Guan and Han 2020; Olcum et al. 2020b). In physiological states, intracellular protein levels of NLRP3, IL-1beta, and IL-18 are minimal. Therefore, in our LPS- and ATP-induced model, the priming step is crucial and initiated by binding LPS to TLR4 to activate downstream NF-κB signaling cascade to induce transcriptions of NLRP3, pro-IL-1β, pro-IL-18, and pro-GSDMD (Piancone et al. 2021). Previous studies have reported that RSV inhibited protein levels of NLRP3, Caspase-1, and IL-1β as inflammasome markers (Sui et al. 2016). However, a serious drawback with this report is that the authors did not study whether RSV affected the priming or activation step of the NLRP3 inflammasome. As opposed to the previous report, in our study, we analyzed

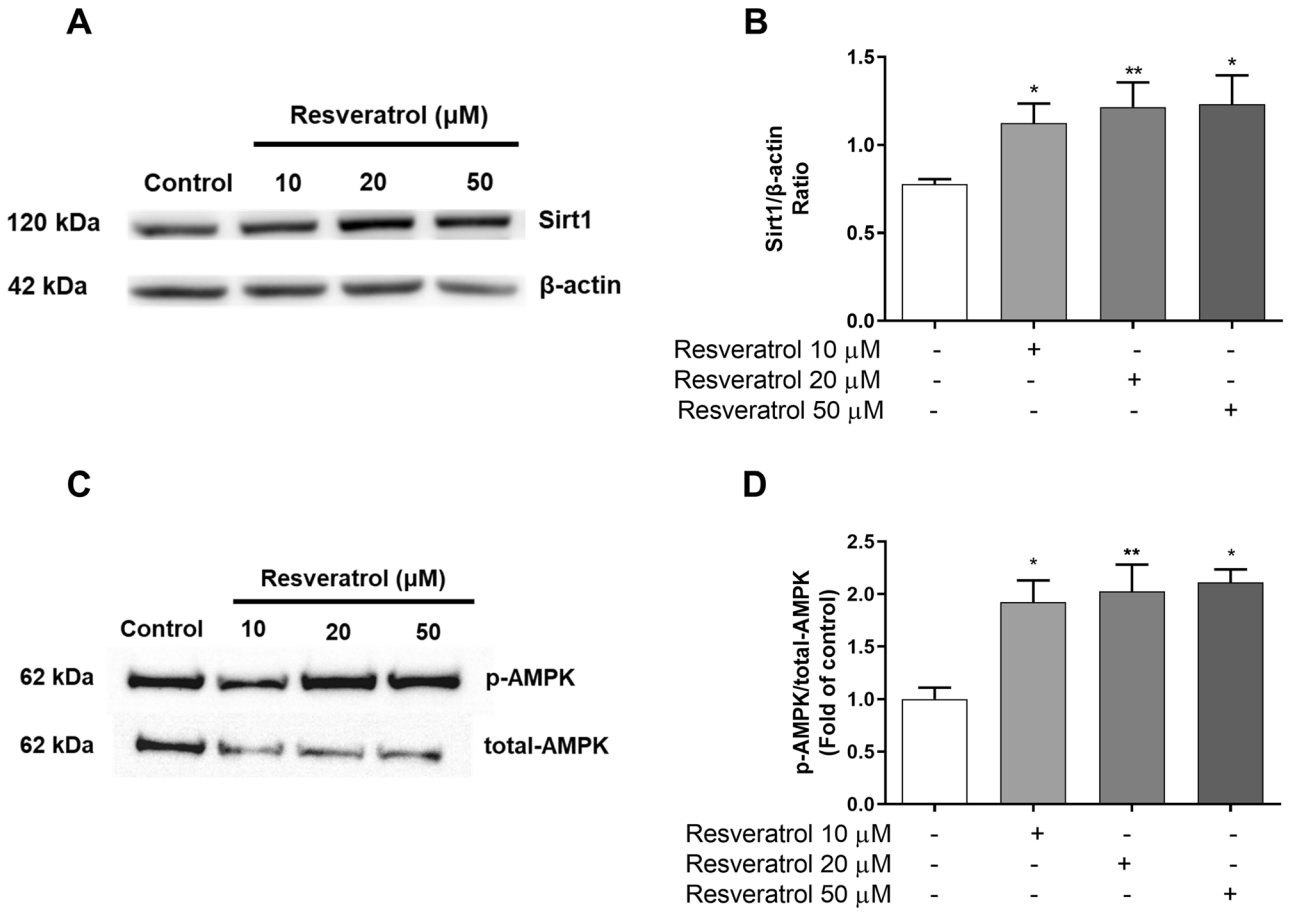

Fig. 6 RSV activated SIRT1 and AMPK pathways. N9 microglial cells were treated with RSV (10 μM, 20 μM, 50 μM) for 0–6 h. (**A**, **B**) RSV pre-treatment activated Sirt1 in a dose-dependent manner. (**C**, **D**) RSV pre-treatment significantly increased phosphorylation of AMPK compared to the untreated cells. The results are presented as mean ± S.E.M, $n = 5$. *$p < 0.05$, **$p < 0.01$ compared to control and #$p < 0.05$, ##$p < 0.01$ compared to LPS- and ATP-treated cells

both mRNA and protein levels of NLRP3 inflammasome components and their transcriptional regulator NF-κB. Hence, these results offer indisputable evidence for the transcriptional regulatory mechanism of RSV on microglial inflammasome activation.

The activation of NLRP3 inflammasome leads to a type of cell death, namely pyroptosis, due to DAMP molecules, such as ATP (Voet et al. 2019). Also, mature caspase-1 mediates cleavage of GSDMD, which then forms pore complexes at the plasma membrane, leading to pyroptotic cell death (Shi et al. 2017). Accumulating evidence has shown that RSV has protective roles against pyroptosis in macrophages and kidney tissues. In studies with macrophages, RSV has been reported to inhibit paclitaxel- or LPS- and ATP-induced pyroptosis by PI staining, without any direct effect of RSV on GSDMD cleavage (Zeng et al. 2019; Chang et al. 2015). Furthermore, in the diabetic ischemia–reperfusion rodent model, RSV has suppressed renal ischemia-associated pyroptosis (Zhang et al. 2020). Our findings have also displayed that RSV inhibited pyroptosis by inhibiting GSDMD cleavage induced by LPS and ATP. Thus, our study demonstrated that RSV inhibited pyroptotic cell death in microglia for the first time in the literature.

RSV has been reported to mediate cellular responses via the AMPK pathway, which is activated due to elevation in cellular AMP/ATP ratio because of stress or starvation. In addition to metabolic functions, AMPK is also associated with cell survival and proliferation. The first investigations into AMPK found that induction of inflammasome by ATP was linked to the AMPK pathway in macrophages (Zha et al. 2016). Furthermore, RSV has been demonstrated to induce autophagy in peritoneal mesothelial cells, which prevented sensitization to NLRP3 inflammasome activation via activation of AMPK signaling (Wu et al. 2016). In other studies, RSV attenuated NLRP3 inflammasome activation in endoplasmic reticulum stress model in adipose tissue (Li et al. 2016), high-glucose-induced inflammasome activation in retinal vascular endothelial cells (Jiang et al. 2019),

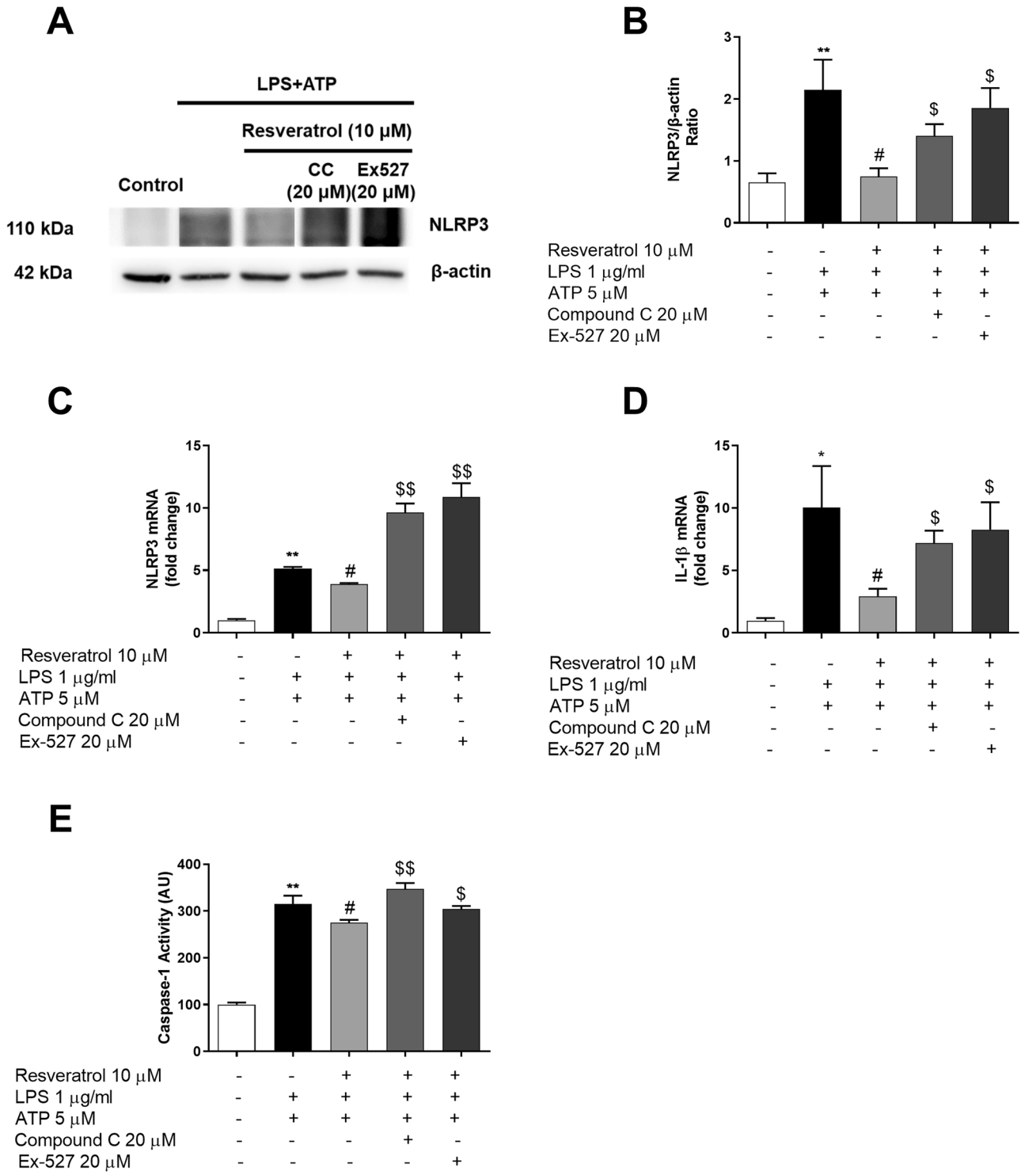

Fig. 7 Inhibition of SIRT1 and AMPK activation ameliorated protective effects by RSV against NLRP3 inflammasome activation. N9 microglial cells were pretreated with CC (20 μM) and Ex527 (20 μM) for 1 h before 1 h RSV (10 μM) pretreatmet, then treated with LPS (1 μg/ml) for 4 h and ATP (5 mM) for 1 h. RSV suppressed NLRP3 inflammasome. CC and Ex527 mediated AMPK and Sirt1 inhibition reversed the protective effect of RSV against (**A**, **B**) NLRP3 protein level, (**C**) NLRP3 mRNA level, (**D**) Il-1β mRNA level, (**E**) caspase-1 activity. The results are presented as mean ± S.E.M, $n = 5$. *$p < 0.05$, **$p < 0.01$ compared to control, #$p < 0.05$, ##$p < 0.01$ compared to LPS- and ATP-treated cells and \$$p < 0.05$, \$\$$p < 0.01$ compated to RSV pretreated cells

and chronic intermittent hypoxia in cardiac tissue (Sun et al. 2020). RSV also protected from amyloid-β-induced neuroinflammation in the hippocampus and prefrontal cortex via activation of AMPK signaling (Qi et al. 2019). Accumulating evidence suggests that RSV caused activation of AMPK, which led to cytoprotective effects in microglia and macrophages (Han et al. 2014; Yi et al. 2011). Moreover, activation of AMPK was suggested to induce the Sirt1 pathway via elevation of intracellular NAD^+ levels (Mancuso et al. 2014), which has therapeutic effects against neurodegeneration and aging (Mancuso et al. 2014). RSV also activates Sirt1 to modulate several cellular signaling cascades related to anti-inflammatory effects (Li et al. 2014). The first studies on the effects of RSV on Sirt1 found that RSV upregulates Sirt1 levels in a dose-dependent manner (Fu et al. 2013). Since Sirt1 is the primary effector mechanism of RSV function, inhibition of Sirt1 diminished the protective effects of RSV in several in vivo and in vitro models (He et al. 2017; Zou et al. 2018; Sui et al. 2016). In a study by Zhou et al., in which CC and Ex527 were utilized, it was demonstrated that both CC and Ex527 alone have attenuated the NLRP3 and mature IL-1β upregulation (Zhou et al. 2020). In addition, Wang et al. have reported that EX527 significantly upregulated the expression of p-NF-κB and pyroptosis-related proteins, such as NLRP3, cleaved caspase 1, cleaved IL-1β, and GSDMD-N, in LPS- and ATP-treated RAW264.7 macrophages (Wang et al. 2021). Similarly, Wang et al. 2019 has demonstrated that CC alone downregulated the expressions of NLRP3 inflammasome-associated proteins (NLRP3 and cleaved caspase 1) in mice (Wang et al. 2019). Also, they reported that CC reduces the p-AMPK/AMPK ratio. Our study analyzed the roles of the AMPK/Sirt1 axis in the protective effects of RSV on the NLRP3 inflammasome activation. First, we have assessed that RSV treatment resulted in increased AMPK phosphorylation and upregulated Sirt1 in microglial cells. Then, we treated cells with AMPK and Sirt1 inhibitors, which are CC and Ex527, respectively, and the protective roles of RSV on NLRP3 inflammasome activation were investigated. Here, we have found that inhibition of AMPK and Sirt1 with chemical inhibitors reversed protective roles of RSV on inflammasome activation associated increase of NLRP3 and IL-1β levels and caspase-1 activity.

MiRNAs, which are the post-transcriptional regulator of mRNA molecules, may affect the expression of upstream or downstream signaling of inflammasome activation or components of the inflammasome complex itself. Of miRNAs, miR-155 is the regulator of innate immune responses and has been reported to regulate inflammasome signaling. Upon activation of TLR4/NF-κB signaling by LPS, miR-155 is upregulated in microglia (Tufekci et al. 2021). The upregulation of miR-155 could be reversed by various phytochemicals, including RSV. The first investigation into the role of RSV on miR-155 found that RSV inhibited inflammatory responses in monocytes (Tili et al. 2010). Furthermore, a recent study has reported that RSV protected BV-2 microglial cells from LPS-induced inflammation by inhibiting miR-155 and promoting M2 polarization. (Ma et al. 2020). However, no studies have reported on the protective role of RSV on microglial inflammasome activation. Although it is known that RSV suppresses inflammasome and regulates miR-155 in myeloid cells, it also has not been demonstrated how signaling pathways regulate it. Here, we report that RSV has alleviated inflammasome activation-induced upregulation of miR-155 in microglial cells. Furthermore, functional studies with miR-155 mimics have shown that miR-155 inhibition resulted in the reversal of protective roles of RSV in NLRP3 inflammasome activation by affecting NLRP3, IL-1β, and IL-18 levels. In addition to the roles of miR-155 in inflammasome activation, our study provided evidence of transcriptional regulatory elements of RSV on miR-155 expression. We believe that this is the first time that inhibition of Sirt1 and AMPK pathways with chemical inhibitors displayed that RSV downregulated LPS and ATP induced miR-155 levels via AMPK and Sirt1 signaling.

We are aware that our research may have some limitations. Pyroptosis can be diverted into the canonical pathway and non-canonical pathway, and the most important initiator is the NLRP3 inflammasome (Yu et al. 2021). In this study, we only investigated the canonical pyroptosis pathway. Our study utilized the N9 microglial cell line to model inflammasome activation in the brain. N9 cell line was obtained from mouse brain and immortalized by *v-myc* overexpression. They have been reported to share similarities with primary mouse microglia (Righi et al. 1989) regarding cell surface marker expression, immune responses against inflammatory stimuli, and phagocytosis ability (Stansley et al. 2012). Furthermore, using a cell line is advantageous in cost, availability, yield, and homogeneity. On the other hand, one limitation of our study is the lack of in vivo studies. Even though some studies reported changes in transcriptome and proteome, N9 cells have been reported to replace in vivo studies (Henn et al. 2009).

Taken together, our results would seem to suggest that RSV treatment inhibits NLRP3 inflammasome activation, pyroptotic cell death, and miR-155 levels in mouse microglial cell line. Our study is the first study that reveals the protective effects of RSV on pyroptotic cell death. Furthermore, considerable progress has been made concerning the mechanism of RSV in microglial cells by determining the roles of Sirt1 and AMPK.

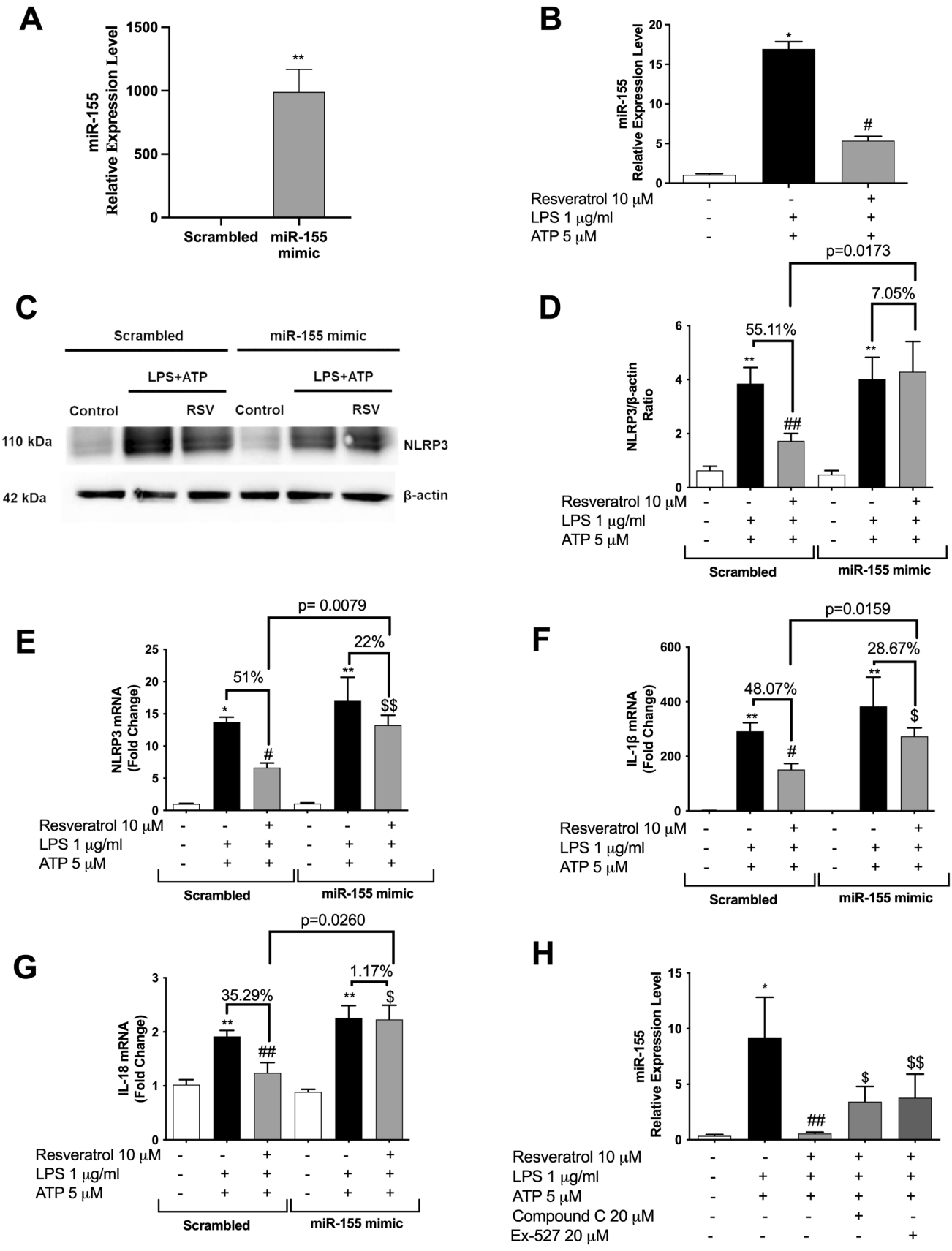
A
miR-155 Relative Expression Level
1500
1000
500
0
**
Scrambled
miR-155 mimic
B
miR-155 Relative Expression Level
20
15
10
5
0
*
#
Resveratrol 10 μM - - +
LPS 1 μg/ml - + +
ATP 5 μM - + +
C
Scrambled
miR-155 mimic
LPS+ATP
LPS+ATP
Control
RSV
Control
RSV
110 kDa
NLRP3
42 kDa
β-actin
D
p=0.0173
7.05%
55.11%
NLRP3/β-actin Ratio
6
4
2
0
**
**
##
Resveratrol 10 μM - - + - - +
LPS 1 μg/ml - + + - + +
ATP 5 μM - + + - + +
Scrambled
miR-155 mimic
E
p= 0.0079
22%
51%
NLRP3 mRNA (Fold Change)
25
20
15
10
5
0
*
**
#
$$
Resveratrol 10 μM - - + - - +
LPS 1 μg/ml - + + - + +
ATP 5 μM - + + - + +
Scrambled
miR-155 mimic
F
p=0.0159
28.67%
48.07%
IL-1β mRNA (Fold Change)
600
400
200
0
**
**
#
$
Resveratrol 10 μM - - + - - +
LPS 1 μg/ml - + + - + +
ATP 5 μM - + + - + +
Scrambled
miR-155 mimic
G
p=0.0260
1.17%
35.29%
IL-18 mRNA (Fold Change)
3
2
1
0
**
**
##
$
Resveratrol 10 μM - - + - - +
LPS 1 μg/ml - + + - + +
ATP 5 μM - + + - + +
Scrambled
miR-155 mimic
H
miR-155 Relative Expression Level
15
10
5
0
*
##
$
$$
Resveratrol 10 μM - - + + +
LPS 1 μg/ml - + + + +
ATP 5 μM - + + + +
Compound C 20 μM - - - + -
Ex-527 20 μM - - - - +

◂**Fig. 8** miR-155 modulates the protective role of RSV in inflammasome activation through Sirt1/AMPK pathway. Transfection efficiency was determined by qPCR. (**A**) miR-155 mimic transfection upregulated miR-155 over 1000 fold compared to the scrambled group.N9 cells were treated with mimic-miR-155 before RSV (10 μM) for 1 h, then treated with LPS (1 μg/ml) for 4 h and ATP (5 mM) for 1 h. miR-155 level was analyzed with qPCR. (**B**) miR-155 expression without any modification upregulated in LPS- and ATP-treated group and downregulated in the RSV pre-treatment group. (**C**, **D**, **E**) After mir-155 activation, the difference in NLRP3 between the LPS and ATP and RSV pre-treatment groups decreased. (**F**) After mir-155 activation, the difference in IL-1β between the LPS and ATP group and RSV pre-treatment group was decreased. (**G**) After mir-155 activation, the difference in IL-18 between the LPS and ATP group and the RSV pre-treatment group was decreased. (**H**) miR-155 mRNA levels measured with and without AMPK/Sirt1 inhibitors. Pre-treatment with CC and Ex527 reversed the downregulation of miR-155 expression significantly compared to the RSV pre-treated cells. The results are presented as mean ± S.E.M, $n=5$. *$p<0.05$, **$p<0.01$ compared to control, #$p<0.05$, ##$p<0.01$ compared to LPS- and ATP-treated cells and \$$p<0.05$, \$\$$p<0.01$ compared to RSV pretreated cells

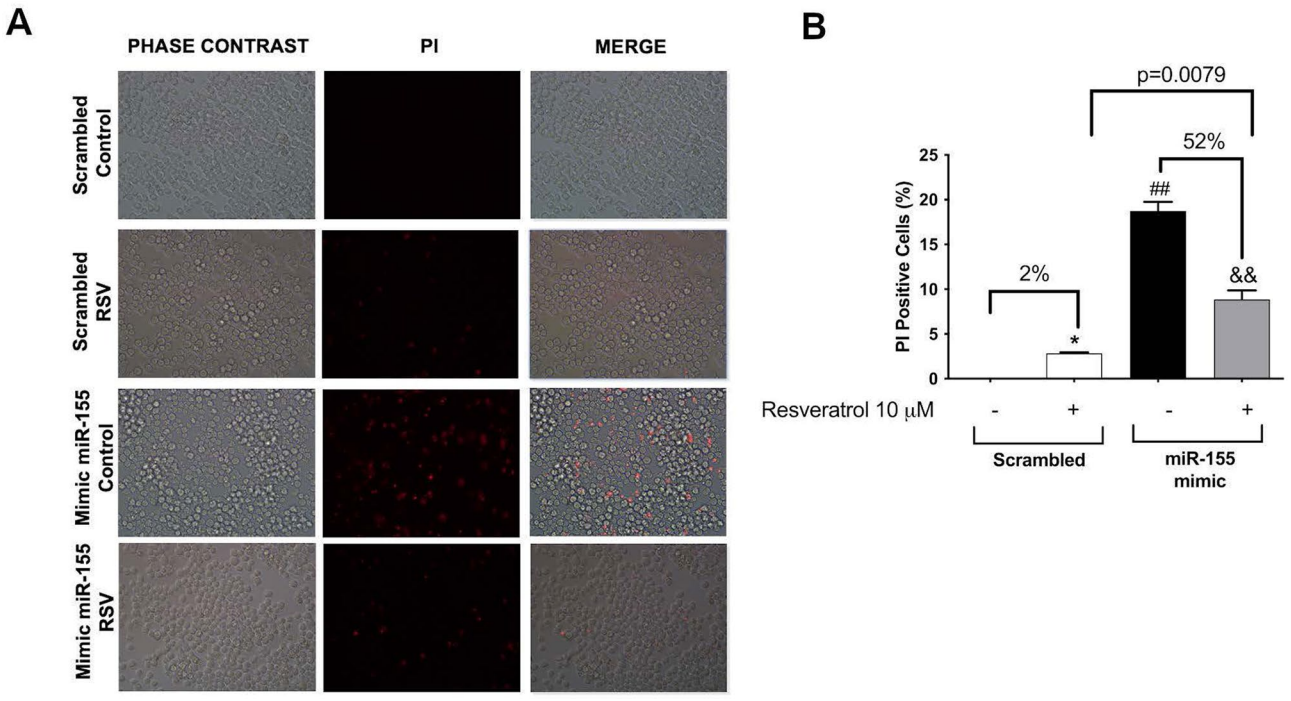

Fig. 9 RSV treatment rescued miR-155 related pyroptotic cell death. N9 cells were treated with mimic-miR-155 before RSV (10 μM) for 1 h. (**A**, **B**) miR-155 transfection increased cell death. RSV prevented pyroptotic cell death and decreased PI-positive cells. The results are presented as mean ± S.E.M, $n=5$. *$p<0.05$, **$p<0.01$ compared to control, #$p<0.05$, ##$p<0.01$ compared to scrambled and \$$p<0.05$, \$\$$p<0.01$ compared to RSV pretreated cells

Author Contribution Conceptualization: Kemal Ugur Tufekci, Sermin Genc. Methodology: Kemal Ugur Tufekci, Bedir Irem Eltutan, Sermin Genc. Formal analysis and investigation: Kemal Ugur Tufekci, Bedir Irem Eltutan, Kamer Burak Isci. Visualization: Kemal Ugur Tufekci, Bedir Irem Eltutan, Kamer Burak Isci. Writing—original draft preparation: Kemal Ugur Tufekci, Bedir Irem Eltutan. Writing—review and editing: Sermin Genc. Funding acquisition: Sermin Genc. Supervision: Sermin Genc.

Funding This work was supported by Dokuz Eylul University (Grant number: 2014.KB.SAG.31).

Declarations

Conflict of Interest The authors declare no competing interests.

References

Artlett CM, Sassi-Gaha S, Hope JL, Feghali-Bostwick CA, Katsikis PD (2017) Mir-155 is overexpressed in systemic sclerosis fibroblasts and is required for NLRP3 inflammasome-mediated collagen synthesis during fibrosis. Arthritis Res Ther 19:144. https://doi.org/10.1186/s13075-017-1331-z

Bauernfeind F, Rieger A, Schildberg FA, Knolle PA, Schmid-Burgk JL, Hornung V (2012) NLRP3 inflammasome activity is negatively controlled by miR-223. J Immunol 189:4175–4181. https://doi.org/10.4049/jimmunol.1201516

Cardoso AL, Guedes JR, de Lima MC (2016) Role of microRNAs in the regulation of innate immune cells under neuroinflammatory conditions. Curr Opin Pharmacol 26:1–9. https://doi.org/10.1016/j.coph.2015.09.001

Chang YP, Ka SM, Hsu WH, Chen A, Chao LK, Lin CC, Hsieh CC, Chen MC, Chiu HW, Ho CL, Chiu YC, Liu ML, Hua KF (2015) Resveratrol inhibits NLRP3 inflammasome activation by preserving mitochondrial integrity and augmenting autophagy. J Cell Physiol 230:1567–1579. https://doi.org/10.1002/jcp.24903

Chen X, He WT, Hu L, Li J, Fang Y, Wang X, Xu X, Wang Z, Huang K, Han J (2016) Pyroptosis is driven by non-selective gasdermin-D pore and its morphology is different from MLKL channel-mediated necroptosis. Cell Res 26:1007–1020. https://doi.org/10.1038/cr.2016.100

Erson-Bensan AE (2014) Introduction to microRNAs in biological systems. In: miRNomics: MicroRNA Biology and Computational Analysis. Springer, pp 1–14. https://doi.org/10.1007/978-1-62703-748-8_1

Espinoza JL, Trung LQ, Inaoka PT, Yamada K, An DT, Mizuno S, Nakao S, Takami A (2017) The repeated administration of resveratrol has measurable effects on circulating T-cell subsets in humans. Oxid Med Cell Longev 2017:6781872. https://doi.org/10.1155/2017/6781872

Feng L, Zhang L (2019) Resveratrol suppresses Abeta-induced microglial activation through the TXNIP/TRX/NLRP3 signaling pathway. DNA Cell Biol 38:874–879. https://doi.org/10.1089/dna.2018.4308

Fu Y, Wang Y, Du L, Xu C, Cao J, Fan T, Liu J, Su X, Fan S, Liu Q, Fan F (2013) Resveratrol inhibits ionising irradiation-induced inflammation in MSCs by activating SIRT1 and limiting NLRP-3 inflammasome activation. Int J Mol Sci 14:14105–14118. https://doi.org/10.3390/ijms140714105

Ghazavi H, Shirzad S, Forouzanfar F, Sahab Negah S, Riyahi Rad M, Vafaee F (2020) The role of resveratrol as a natural modulator in glia activation in experimental models of stroke. Avicenna J Phytomed 10:557–573

Grosshans H, Filipowicz W (2008) Proteomics joins the search for microRNA targets. Cell 134:560–562. https://doi.org/10.1016/j.cell.2008.08.008

Guan Y, Han F (2020) Key mechanisms and potential targets of the NLRP3 inflammasome in neurodegenerative diseases. Front Integr Neurosci 14:37. https://doi.org/10.3389/fnint.2020.00037

Han Y, Jiang C, Tang J, Wang C, Wu P, Zhang G, Liu W, Jamangulova N, Wu X, Song X (2014) Resveratrol reduces morphine tolerance by inhibiting microglial activation via AMPK signalling. Eur J Pain 18:1458–1470. https://doi.org/10.1002/ejp.511

Hanamsagar R, Hanke ML, Kielian T (2012) Toll-like receptor (TLR) and inflammasome actions in the central nervous system. Trends Immunol 33:333–342. https://doi.org/10.1016/j.it.2012.03.001

He Q, Li Z, Wang Y, Hou Y, Li L, Zhao J (2017) Resveratrol alleviates cerebral ischemia/reperfusion injury in rats by inhibiting NLRP3 inflammasome activation through Sirt1-dependent autophagy induction. Int Immunopharmacol 50:208–215. https://doi.org/10.1016/j.intimp.2017.06.029

Heneka MT, McManus RM, Latz E (2018) Inflammasome signalling in brain function and neurodegenerative disease. Nat Rev Neurosci 19:610–621. https://doi.org/10.1038/s41583-018-0055-7

Henn A, Lund S, Hedtjarn M, Schrattenholz A, Porzgen P, Leist M (2009) The suitability of BV2 cells as alternative model system for primary microglia cultures or for animal experiments examining brain inflammation. ALTEX 26:83–94. https://doi.org/10.14573/altex.2009.2.83

Herman FJ, Pasinetti GM (2018) Principles of inflammasome priming and inhibition: Implications for psychiatric disorders. Brain Behav Immun 73:66–84. https://doi.org/10.1016/j.bbi.2018.06.010

Hung WL, Ho CT, Pan MH (2020) Targeting the NLRP3 inflammasome in neuroinflammation: health promoting effects of dietary phytochemicals in neurological disorders. Mol Nutr Food Res 64:e1900550. https://doi.org/10.1002/mnfr.201900550

Jiang T, Gu J, Chen W, Chang Q (2019) Resveratrol inhibits high-glucose-induced inflammatory "metabolic memory" in human retinal vascular endothelial cells through SIRT1-dependent signaling. Can J Physiol Pharmacol 97:1141–1151. https://doi.org/10.1139/cjpp-2019-0201

Kaufmann FN, Costa AP, Ghisleni G, Diaz AP, Rodrigues ALS, Peluffo H, Kaster MP (2017) NLRP3 inflammasome-driven pathways in depression: clinical and preclinical findings. Brain Behav Immun 64:367–383. https://doi.org/10.1016/j.bbi.2017.03.002

Lee G, Park JS, Lee EJ, Ahn JH, Kim HS (2019) Anti-inflammatory and antioxidant mechanisms of urolithin B in activated microglia. Phytomedicine : International Journal of Phytotherapy and Phytopharmacology 55:50–57. https://doi.org/10.1016/j.phymed.2018.06.032

Li A, Zhang S, Li J, Liu K, Huang F, Liu B (2016) Metformin and resveratrol inhibit Drp1-mediated mitochondrial fission and prevent ER stress-associated NLRP3 inflammasome activation in the adipose tissue of diabetic mice. Mol Cell Endocrinol 434:36–47. https://doi.org/10.1016/j.mce.2016.06.008

Li XM, Zhou MT, Wang XM, Ji MH, Zhou ZQ, Yang JJ (2014) Resveratrol pretreatment attenuates the isoflurane-induced cognitive impairment through its anti-inflammation and -apoptosis actions in aged mice. J Mol Neurosci 52:286–293. https://doi.org/10.1007/s12031-013-0141-2

Liu T, Ma Y, Zhang R, Zhong H, Wang L, Zhao J, Yang L, Fan X (2019) Resveratrol ameliorates estrogen deficiency-induced depression- and anxiety-like behaviors and hippocampal inflammation in mice. Psychopharmacology 236:1385–1399. https://doi.org/10.1007/s00213-018-5148-5

Livak KJ, Schmittgen TD (2001) Analysis of relative gene expression data using real-time quantitative PCR and the 2(-Delta Delta

C(T)) Method. Methods 25:402–408. https://doi.org/10.1006/meth.2001.1262
Lu X, Ma L, Ruan L, Kong Y, Mou H, Zhang Z, Wang Z, Wang JM, Le Y (2010) Resveratrol differentially modulates inflammatory responses of microglia and astrocytes. J Neuroinflammation 7:46. https://doi.org/10.1186/1742-2094-7-46
Ma S, Fan L, Li J, Zhang B, Yan Z (2020) Resveratrol promoted the M2 polarization of microglia and reduced neuroinflammation after cerebral ischemia by inhibiting miR-155. Int J Neurosci 130:817–825. https://doi.org/10.1080/00207454.2019.1707817
Mancuso R, del Valle J, Modol L, Martinez A, Granado-Serrano AB, Ramirez-Nunez O, Pallas M, Portero-Otin M, Osta R, Navarro X (2014) Resveratrol improves motoneuron function and extends survival in SOD1(G93A) ALS mice. Neurotherapeutics : the Journal of the American Society for Experimental NeuroTherapeutics 11:419–432. https://doi.org/10.1007/s13311-013-0253-y
Movahed A, Nabipour I, Lieben Louis X, Thandapilly SJ, Yu L, Kalantarhormozi M, Rekabpour SJ, Netticadan T (2013) Antihyperglycemic effects of short term resveratrol supplementation in type 2 diabetic patients. Evid Based Complement Alternat Med 2013:851267. https://doi.org/10.1155/2013/851267
O'Connell RM, Taganov KD, Boldin MP, Cheng GH, Baltimore D (2007) MicroRNA-155 is induced during the macrophage inflammatory response. Proc Natl Acad Sci USA 104:1604–1609. https://doi.org/10.1073/pnas.0610731104
Olcum M, Tastan B, Ercan I, Eltutan IB, Genc S (2020a) Inhibitory effects of phytochemicals on NLRP3 inflammasome activation: a review. Phytomedicine : International Journal of Phytotherapy and Phytopharmacology 75:153238. https://doi.org/10.1016/j.phymed.2020.153238
Olcum M, Tastan B, Kiser C, Genc S, Genc K (2020b) Microglial NLRP3 inflammasome activation in multiple sclerosis. Adv Protein Chem Struct Biol 119:247–308. https://doi.org/10.1016/bs.apcsb.2019.08.007
Piancone F, Rosa La F, Marventano I, Saresella M, Clerici M (2021) The role of the inflammasome in neurodegenerative diseases. Molecules 26. https://doi.org/10.3390/molecules26040953
Qi Y, Shang L, Liao Z, Su H, Jing H, Wu B, Bi K, Jia Y (2019) Intracerebroventricular injection of resveratrol ameliorated Abeta-induced learning and cognitive decline in mice. Metab Brain Dis 34:257–266. https://doi.org/10.1007/s11011-018-0348-6
Righi M, Mori L, De Libero G, Sironi M, Biondi A, Mantovani A, Donini SD, Ricciardi-Castagnoli P (1989) Monokine production by microglial cell clones. Eur J Immunol 19:1443–1448. https://doi.org/10.1002/eji.1830190815
Schindelin J, Rueden CT, Hiner MC, Eliceiri KW (2015) The ImageJ ecosystem: an open platform for biomedical image analysis. Mol Reprod Dev 82:518–529. https://doi.org/10.1002/mrd.22489
Schneider CA, Rasband WS, Eliceiri KW (2012) NIH Image to ImageJ: 25 years of image analysis. Nat Methods 9:671–675. https://doi.org/10.1038/nmeth.2089
Shi J, Gao W, Shao F (2017) Pyroptosis: gasdermin-mediated programmed necrotic cell death. Trends Biochem Sci 42:245–254. https://doi.org/10.1016/j.tibs.2016.10.004
Shi J, Zhao Y, Wang K, Shi X, Wang Y, Huang H, Zhuang Y, Cai T, Wang F, Shao F (2015) Cleavage of GSDMD by inflammatory caspases determines pyroptotic cell death. Nature 526:660–665. https://doi.org/10.1038/nature15514
Stansley B, Post J, Hensley K (2012) A comparative review of cell culture systems for the study of microglial biology in Alzheimer's disease. J Neuroinflammation 9:115. https://doi.org/10.1186/1742-2094-9-115
Sui DM, Xie Q, Yi WJ, Gupta S, Yu XY, Li JB, Wang J, Wang JF, Deng XM (2016) Resveratrol protects against sepsis-associated encephalopathy and inhibits the NLRP3/IL-1beta axis in microglia. Mediators Inflamm 2016:1045657. https://doi.org/10.1155/2016/1045657
Sun ZM, Guan P, Luo LF, Qin LY, Wang N, Zhao YS, Ji ES (2020) Resveratrol protects against CIH-induced myocardial injury by targeting Nrf2 and blocking NLRP3 inflammasome activation. Life Sci 245:117362. https://doi.org/10.1016/j.lfs.2020.117362
Tang Y, Le W (2016) Differential roles of M1 and M2 microglia in neurodegenerative diseases. Mol Neurobiol 53:1181–1194. https://doi.org/10.1007/s12035-014-9070-5
Thiel G, Rossler OG (2016) Resveratrol stimulates cyclic AMP response element mediated gene transcription. Mol Nutr Food Res 60:256–265. https://doi.org/10.1002/mnfr.201500607
Tili E, Michaille J-J, Cimino A, Costinean S, Dumitru CD, Adair B, Fabbri M, Alder H, Liu CG, Calin GA (2007) Modulation of miR-155 and miR-125b levels following lipopolysaccharide/TNF-α stimulation and their possible roles in regulating the response to endotoxin shock. J Immunol 179:5082–5089. https://doi.org/10.4049/jimmunol.179.8.5082
Tili E, Michaille JJ, Adair B, Alder H, Limagne E, Taccioli C, Ferracin M, Delmas D, Latruffe N, Croce CM (2010) Resveratrol decreases the levels of miR-155 by upregulating miR-663, a microRNA targeting JunB and JunD. Carcinogenesis 31:1561–1566. https://doi.org/10.1093/carcin/bgq143
Tufekci KU, Ercan I, Isci KB, Olcum M, Tastan B, Gonul CP, Genc K, Genc S (2021) Sulforaphane inhibits NLRP3 inflammasome activation in microglia through Nrf2-mediated miRNA alteration. Immunol Lett 233:20–30. https://doi.org/10.1016/j.imlet.2021.03.004
Tufekci KU, Meuwissen RL, Genc S (2014) The role of microRNAs in biological processes. Methods Mol Biol 1107:15–31. https://doi.org/10.1007/978-1-62703-748-8_2
Turner RS, Thomas RG, Craft S, van Dyck CH, Mintzer J, Reynolds BA, Brewer JB, Rissman RA, Raman R, Aisen PS, Alzheimer's Disease Cooperative S (2015) A randomized, double-blind, placebo-controlled trial of resveratrol for Alzheimer disease. Neurology 85:1383–1391. https://doi.org/10.1212/WNL.0000000000002035
Voet S, Srinivasan S, Lamkanfi M, van Loo G (2019) Inflammasomes in neuroinflammatory and neurodegenerative diseases. EMBO Mol Med 11. https://doi.org/10.15252/emmm.201810248
Walter J, Kemmerling N, Wunderlich P, Glebov K (2017) γ-Secretase in microglia–implications for neurodegeneration and neuroinflammation. J Neurochem 143:445–454. https://doi.org/10.1111/jnc.14224
Wang F, Liu Y, Yuan J, Yang W, Mo Z (2019) Compound C protects mice from HFD-induced obesity and nonalcoholic fatty liver disease. Int J Endocrinol 2019:3206587. https://doi.org/10.1155/2019/3206587
Wang Y, Wang Y, Cai N, Xu T, He F (2021) Anti-inflammatory effects of curcumin in acute lung injury: In vivo and in vitro experimental model studies. Int Immunopharmacol 96:107600. https://doi.org/10.1016/j.intimp.2021.107600
Wu J, Li X, Zhu G, Zhang Y, He M, Zhang J (2016) The role of Resveratrol-induced mitophagy/autophagy in peritoneal mesothelial cells inflammatory injury via NLRP3 inflammasome activation triggered by mitochondrial ROS. Exp Cell Res 341:42–53. https://doi.org/10.1016/j.yexcr.2016.01.014
Yi CO, Jeon BT, Shin HJ, Jeong EA, Chang KC, Lee JE, Lee DH, Kim HJ, Kang SS, Cho GJ, Choi WS, Roh GS (2011) Resveratrol activates AMPK and suppresses LPS-induced NF-kappaB-dependent COX-2 activation in RAW 264.7 macrophage cells. Anat Cell Biol 44:194–203. https://doi.org/10.5115/acb.2011.44.3.194
Yu P, Zhang X, Liu N, Tang L, Peng C, Chen X (2021) Pyroptosis: mechanisms and diseases. Signal Transduct Target Ther 6:128. https://doi.org/10.1038/s41392-021-00507-5
Zeng QZ, Yang F, Li CG, Xu LH, He XH, Mai FY, Zeng CY, Zhang CC, Zha QB, Ouyang DY (2019) Paclitaxel enhances the innate

immunity by promoting NLRP3 inflammasome activation in macrophages. Front Immunol 10:72. https://doi.org/10.3389/fimmu.2019.00072

Zha QB, Wei HX, Li CG, Liang YD, Xu LH, Bai WJ, Pan H, He XH, Ouyang DY (2016) ATP-induced inflammasome activation and pyroptosis is regulated by AMP-activated protein kinase in macrophages. Front Immunol 7:597. https://doi.org/10.3389/fimmu.2016.00597

Zhang J, Wang L, Gong D, Yang Y, Liu X, Chen Z (2020) Inhibition of the SIRT1 signaling pathway exacerbates endoplasmic reticulum stress induced by renal ischemia/reperfusion injury in type 1 diabetic rats. Mol Med Rep 21:695–704. https://doi.org/10.3892/mmr.2019.10893

Zhang X, Wu Q, Zhang Q, Lu Y, Liu J, Li W, Lv S, Zhou M, Zhang X, Hang C (2017) Resveratrol attenuates early brain injury after experimental subarachnoid hemorrhage via inhibition of NLRP3 inflammasome activation. Front Neurosci 11:611. https://doi.org/10.3389/fnins.2017.00611

Zhou B, Qiu Y, Wu N, Chen AD, Zhou H, Chen Q, Kang YM, Li YH, Zhu GQ (2020) FNDC5 attenuates oxidative stress and NLRP3 inflammasome activation in vascular smooth muscle cells via activating the AMPK-SIRT1 signal pathway. Oxid Med Cell Longev 2020:6384803. https://doi.org/10.1155/2020/6384803

Zou P, Liu X, Li G, Wang Y (2018) Resveratrol pretreatment attenuates traumatic brain injury in rats by suppressing NLRP3 inflammasome activation via SIRT1. Mol Med Rep 17:3212–3217. https://doi.org/10.3892/mmr.2017.8241